# Seismic Robustness Assessment of Code Compliant Steel Moment Resisting Frame Under Seismic Triggered Sequences of Events

**Filipe L. A. Ribeiro & Luís C. Neves**
*UNIC, Faculdade de Ciências e Tecnologia, Universidade Nova de Lisboa, Portugal*

**André R. Barbosa**
*School of Civil and Construction Engineering, Oregon State University, Corvallis, U.S.A.*

15 WCEE
LISBOA 2012

**SUMMARY:**
Earthquakes cannot be seen as isolated hazard events. High intensity earthquakes usually lead to secondary hazard events, such as fire, blasts, aftershocks and tsunamis, whose consequences have significant impact on life safety in post-mainshock risk scenarios. These secondary events that follow major earthquakes are not considered in codes. In this study, a probabilistic framework for evaluation of the structural safety under sequences of events is presented. After quantifying the structural safety, considering two specific seismic triggered sequences of events, and comparing it to that associated with the mainshock alone, a measure of the structural robustness to cascading events can be defined, independently of current life safety requirements present in codes. A newly designed steel frame building to be located in Lisbon, Portugal, is used as a case study. A nonlinear finite element model accounting for cyclic deterioration is developed in OpenSees. Code spectra compatible ground motions are used through spectrum matching of historical earthquake records using a wavelet-based transformation method.

*Keywords: Aftershocks, Element removal, Nonlinear Dynamic Analysis, Robustness, Sequences of Events*

## 1. INTRODUCTION

In the aftermath of a strong earthquake, secondary events such as fire, blasts, aftershocks and tsunamis, bring additional risk of failure to the buildings already damaged by the original earthquake. These events can have a significant impact on life safety (as well as collapse prevention) and on structural resiliency (ability of the structure to regain its functionality after the mainshock). However, design of new buildings according to current codes (e.g. IPQ (2010b) and JCSS (2001)) does not consider cascading events that follow a major earthquake.

Structural safety considering sequences of events associated with a mainshock and subsequent events are analyzed herein through the development of a probabilistic methodological framework that allows for the quantification of the safety of the structure under each sequence of mainshock triggered sequence of events. Two specific situations are addressed in this study: (i) mainshock followed by aftershock, and (ii) mainshock followed by fire or blast that induces localized damage on the structure (which can lead to partial collapse) and then followed by an aftershock. Through quantification of the structural safety under a mainshock alone and comparing it with the safety associated with these sequences of events, it is possible to assess the robustness in these scenarios.

To demonstrate the applicability of the proposed framework, a case study, consisting in a steel frame building located in Lisbon, Portugal, is used considering the two sequences of events described above. Structural analysis of the building is performed in the Open System for Earthquake Engineering Simulation software (OpenSees) (Mazzoni et al., 2009), using a nonlinear finite element model which accounts for cyclic deterioration of components (beams and columns). The model is intended to capture progressive collapse situations that result from propagation of localized damage on the structure. Model parameters of moment-rotation relationships of the plastic hinge regions, including the ones associated with the deterioration modes considered, are estimated through empirical relationships developed by Lignos (2008) and Lignos and Krawinkler (2011), which resulted from statistical treatment of hundreds of experimental tests performed over the last decades.

A sequence of nonlinear dynamic time-history response analyses are performed using modified historical ground motions records. The historical earthquake records were obtained from the PEER NGA database (PEER, 2007). The ground motion response spectra were modified, using a wavelet-based transformation method (Mukherjee and Gupta, 2002), to match the EC8 (IPQ (2010b) and Campos Costa et al. (1998)) code spectra for Lisbon, Portugal. In the development of the probability distributions, spectral accelerations are assumed to follow a log-normal distribution (Jayaram and Baker, 2008).

With the framework proposed in this study, it is possible to: (i) assess the risk associated with sequences of events following a major earthquake, (ii) compare this risk with that associated with the mainshock alone, and, in the near future, to (iii) define structural types more robust to cascading events.

## 2. PREVIOUS RESEARCH AND DEVELOPMENTS

In the last decades, much importance has been given to the seismic risk decision making process. In that context one of the main developments was the creation of a probabilistic framework that provides assessment and design methods for risk analysis. The *Performance-based Earthquake Engineering* (PBEE) (Moehle and Deierlein, 2004) approach is divided in four main steps, each requiring inputs from different disciplines. Firstly, through probabilistic seismic hazard analyses (PSHA) (McGuire, 2004), it is possible to probabilistically define the ground motions through the so-called Intensity Measures (*IM*) (e.g., the peak ground acceleration or spectral acceleration). Second, (nonlinear) structural analysis is used to study the structural response under the seismic actions defined by *IM*, which is generally described through Engineering Demand Parameters (*EDP*). For buildings, these parameters can be deformations, accelerations, forces, interstory drifts, among others. The correlation between *IM* and *EDP* is generally assessed using incremental dynamic analysis (IDA) (Vamvatsikos and Cornell, 2002). Third, the next step in the PBEE process is to perform a damage analysis, which relates the *EDP* values to Damage Measures *(DM)*, at different Damage States *(DS)*, which in turn describe the physical damage of a facility. The final step in the assessment is to calculate Decision Variables *(DV)*, in terms that are meaningful for decision makers (generally, direct dollar losses, downtime or restoration time, and casualties).

The application of the PBEE methodology has been used in the assessment of structural safety for mainshock scenarios (Bazzurro et al., 2006). However, due to its flexibility it is possible to consider other events that may have significant impact in the *DV* computation, especially in post-mainshock risk scenarios. Mainshock triggered hazard events, such as aftershocks (Yeo and Cornell (2005) and Luco et al. (2011a)) and fire following earthquakes (Braxtan and Pessiki, 2011) are important and should be included in these type of analysis.

Regarding to the aftershocks, although their intensity is usually smaller than the mainshock intensity, their consequences can be larger than expected as structures may already be damaged by the mainshock. Thus, post-mainshock structural resistant capacity should be considered a random variable in the analysis of these scenarios. In fact, Luco et al. (2004, 2011b) defined this random residual capacity in terms of the smallest spectral acceleration that would induce localized or complete collapse in an aftershock. The introduction of the aftershocks in the PBEE has led to a new framework called *Aftershock Performance-Based Earthquake Engineering* (APBEE) (Yeo and Cornell, 2005).

The study of structural post-mainshock behavior (i.e. aftershock fragility) has gained more relevance in the past few years. Using IDA with a sequence of mainshock-aftershock ground motions, Luco et al. (2011b) presented some relations that define the probability that a structure, in a certain damage state has, in exceeding a higher damage state due to an aftershock.

Besides the aftershocks, up to date and to the authors knowledge there have not been any other developments aiming at accounting for performance-based engineering efforts that also account for other seismic triggered events that may follow a mainshock. Although some recent studies (e.g. Braxtan and Pessiki (2011)) have addressed the fire post-earthquake issue, its introduction in a probabilistic framework has not been attempted to our knowledge.

## 3. ROBUSTNESS ASSESSMENT OF STRUCTURES UNDER SEISMIC HAZARDS AND SUBSEQUENT HAZARD EVENTS

### 3.1. General Formulation

The seismic triggered events considered in this study are aftershocks and localized fires and/or blasts. To assess the robustness of structures under seismic sequences of events triggered by a mainshock, a probabilistic methodology is proposed. Robustness is defined herein as the structure capacity to overcome unexpected events with damage which is not disproportional to the one caused by an original hazard event. As a consequence, by comparing the probabilities of collapse associated with different sequences of events and the one associated with the original mainshock event, measures of robustness can be defined. In this study a robustness factor *RF* is proposed that accounts for the probability of collapse for both scenarios that include either the mainshock alone $P(C)_{mainshock}$, or other mainshock triggered events $P(C)_{seq\text{-}events}$. The robustness factor proposed is given by:

$$RF = \left( exp\left( \frac{P(C)_{seq-events} - P(C)_{mainshock}}{P(C)_{mainshock}} \right) \right)^{-1} \tag{3.1}$$

To compute the *RF*, the probabilities of collapse have to be quantified, and these can be given by the following equation:

$$\begin{aligned} P(C) = \int_{S_a{}^m(T_1)} \int_F \int_{DS} \int_{S_a{}^a(T_1)} & P(C \mid sa_1{}^m, sa_1{}^a, ds) \times dP(sa_1{}^a \mid sa_1{}^m) \times dP(ds \mid F) \\ & \times dP(F \mid sa_1{}^m) \times dP(sa_1{}^m) \end{aligned} \tag{3.2}$$

where the spectral acceleration ($S_a(T_1)= sa_1$) at the fundamental period of the structure $T_1$ is considered to characterize the ground motion *IM*; the spectral accelerations $sa_1{}^m$ and $sa_1{}^a$ are associated with the mainshock and the aftershock at the fundamental period of the structure, respectively; *F* corresponds to the occurrence of fire and/or blast following the mainshock; and *ds* is the damage state after both the mainshock and the localized fires and/or blasts have occurred. In this work, the effect of fire/blast in the damage state *ds* is simulated through direct removal of one of more structural elements. In Eqn. 3.2 four conditional probability terms are shown. First, $dP(sa_1{}^a|sa_1{}^m)$ is the representation for $f_{sa_1{}^a|sa_1{}^m}(sa_1{}^a \mid sa_1{}^m)dsa_1{}^a$, which is the conditional probability of occurrence of an aftershock with spectral acceleration value $sa_1{}^a$ given that a mainshock with a spectral acceleration value $sa_1{}^m$ occurred. Second, $dP(ds|F)$ corresponds to the conditional probability of the structure being in certain damage state *ds* as a result of fire and/or blast following earthquake, *F*. Third, $dP(F|\ sa_1{}^m)$ is the probability of occurrence of fire or blast following a mainshock characterized by $sa_1{}^m$. The probability of occurrence of a spectral acceleration associated with the mainshock is denoted by $dP(sa_1{}^m)$. Finally, $P(C|\ sa_1{}^m, sa_1{}^a, ds)$ corresponds to the cumulative probability distribution function of *C* (*structural collapse criteria*) conditional on: (i) a given mainshock $sa_1{}^m$, (ii) a given aftershock $sa_1{}^a$, and (iii) the current damage state, *ds*, which includes both the mainshock and localized damage due to fire/blast. The conditional probability of collapse is given by:

$$P(C \mid sa_1^m, sa_1^a, ds) = P[sa_1^a > sa_1^{a,c} \mid S_a^m(T_1) = sa_1^m, S_a^a(T_1) = sa_1^a, \\ DS = ds] \tag{3.3}$$

where $sa_1^{a,c}$ represents the minimum spectral acceleration of the aftershock leading to collapse defined as the exceedance of one or more structural damage indicators (Faisian et al., 2005).

Each of the components in Eqn. 3.2 requires inputs from a specific discipline (earthquake engineering, structural engineering, fire engineering). It is worth noting that this methodology can be applied to any structural typology or material, since it is possible to define a model that allows tracking the mainshock-damaged behavior.

### 3.2. Simplified Formulation

At this time there is no well established method for characterization of the probability of fire/blast following earthquake. Thus terms of the conditional probability $dP(F| sa_1^m)$ and also the F/DS relationship and its distribution $dP(ds|F)$ shown in Eqn. 3.2 are not currently (to our knowledge) available in literature. As a consequence, the direct application of Eqn. 3.2 is not trivial at this moment. A simplified version of Eqn. 3.2 is presented next in which it is assumed that the damage state $ds$ accounts implicitly for the effects of fire or blast following earthquake:

$$P(C) = \int_{S_a^m(T_1)} \int_{DS} \int_{S_a^a(T_1)} P(C \mid sa_1^m, sa_1^a, ds) \times dP(sa_1^a \mid sa_1^m) \times dP(DS \mid sa_1^m) \\ \times dP(sa_1^m) \tag{3.4}$$

In this context, $dP(DS| sa_1^m)$ is the probability of occurrence of a certain structural damage $ds$ after a mainshock with spectral acceleration $sa_1^m$ and, implicitly accounts also for damages due to fire or blast.

The collapse probability is quantified by the integral of the collapse probability associated to each combination of events, multiplied by the individual probabilities of occurrence. Three different collapse situations are addressed in Eqn. 3.4: (i) collapse is recorded during the mainshock; (ii) after the mainshock fire or blast induces localized damage on the structure which yields in a progressive collapse situation; and (iii) collapse takes place when an aftershock exceeds the residual capacity of the structure already damaged by the mainshock or by the mainshock and the fire/blast.

### 3.3. Methods and application

The simulation of the scenarios considered in this study is only possible by performing nonlinear dynamic time-history response analyses, which were executed in OpenSees (Mazzoni et al., 2009). In these analyses ten modified historical ground motion records obtained from the PEER NGA database (PEER, 2007) were used. The ground motion records were spectrum modified to match, in terms of amplitude and frequency content the EC8 (IPQ (2010b) and Campos Costa et al. (1998)) code spectra for Lisbon, Portugal. A wavelet-based transformation method (Mukherjee and Gupta, 2002) was used to generate code compliant accelerograms. The distribution of the intensity measures was defined by approximating the spectral accelerations with a log-normal distribution (Jayaram and Baker, 2008), which is a common assumption in a conventional probabilistic seismic hazard analysis (PSHA). The two different types of seismic action defined in the EC8: type 1 (high magnitude and distant) and type 2 (lower magnitude but closer epicenter), were considered in the analysis.

In order to perform a finite number of analyses, the $sa_1^m$ values are defined with stratified sampling (Bartlett et al., 2001), dividing the sample space into 18 intervals. The spectral acceleration for the aftershock, $sa_1^a$, is found using directional sampling (Mardia and Jupp, 2000) and the bisection method

(Burden and Faires, 1985). In this manner it is possible, using Eqn. 3.4, to quantify the collapse probability.

Furthermore, the damage induced by a fire/blast is simulated by the direct element removal (Talaat and Mosalam, 2009) of one or more elements, which is implemented during an ongoing analysis within the OpenSees framework. In this study the element removal is performed at each of the columns of the first story level.

Finally, it is important to note some of the assumptions made in this preliminary study: (i) it was assumed that no correlation exists between the spectral accelerations associated with mainshock and the aftershock; (ii) structural properties are assumed to be deterministic and equal to their mean values and uncertainty considered includes the record-to-record variability and the distribution in the ground motion *IM*. The ground motion records are spectrum modified and the *IM* is taken as the spectral acceleration at the fundamental period of vibration of the undamaged structure at its initial state. It is worth noting that since the EC8 definition for the response spectra is used herein and the ground motions are spectrum modified to match the EC8 spectra, the spectral accelerations at different periods are assumed to be perfectly correlated.

MATLAB software was used for the execution of the described formulation. The input data is: mainshock intensity values, structural model properties and parameters and the element to be removed after the mainshock, simulating the damage induced by fire/blast. As referred above, seismic action was defined in terms of the ground motion spectral acceleration probabilistic distribution function corresponding to the first vibration mode of the intact structure (Ribeiro, 2011).

The analysis of each $sa_1^m$ is done performing the nonlinear dynamic time-history response analysis correspondent to the mainshock. If the collapse occurs during the mainshock the analysis is stopped. The damage indicators used to define collapse are the exceedance of 6% of inter-storey drift ratio $(\Delta_{story}/h_{story})$ and/or 4% of the normalized roof displacement $(\Delta_r/H)$. Otherwise, after the mainshock the program proceeds to the removal of one and only one element at the first story level, which corresponds to an element that is assumed to have been completely damaged due to a fire/blast. Immediately after the element removal, nonlinear dynamic time-history response analyses corresponding to the aftershock are performed. These back to back analyses are performed for many $sa_1^a$ values until the minimum aftershock spectral acceleration value $(sa_1^{a,c})$ that leads to the prescribed structural damage indicator has been achieved. This search is performed using the bisection method. Using the analytical approach described in this paragraph the probability of collapse (Eqn. 3.4) can be re-written as:

$$\begin{aligned} P(C) = \sum_{j=1}^{n_{ds}} \sum_{i=1}^{n_{sa_1^m}} & P(sa_1^a > sa_1^{a,c} \mid sa_1^{m,i}, ds^j) \times P(S_a^m(T_1) = sa_1^{m,i}) \\ & \times P(DS = ds^j \mid sa_1^{m,i}) \end{aligned} \tag{3.5}$$

where $sa_1^{m,i}$ is the $i^{th}$ spectral acceleration value associated with the mainshock considered; $ds^j$ is the $j^{th}$ possible scenario of localized damage induced on the structure due to fire/blast; $n_{sa_1^m}$ and $n_{ds^j}$ are the number of mainshock values considered and the number of possible localized damage scenarios (due to fire/blast post-mainshock), respectively. The last term, i.e. the number of possible localized damage scenarios, corresponds to the number of columns of the first story level plus one more scenario where no elements are removed. Three situations are addressed in Eqn. 3.5: (i) the collapse probability is given by $P(S_a^m(T_1)= sa_1^{m,i})$ when collapse occurs during the mainshock; (ii) in the case that progressive collapse takes place after the mainshock due to a localized damage on the structure induced by fire or blasts, the collapse probability is given by $P(S_a^m(T_1)= sa_1^{m,i}).P(DS=ds^j|sa_1^{m,i})$, and finally (iii) collapse can occur when the aftershock spectral acceleration, $sa_1^a$, is larger than the minimum value that leads to collapse, $sa_1^{a,c}$. After analyzing all the considered $S_a^m(T_1)$ values and all risk scenarios, the probabilities of collapse are computed using Eqn. 3.5. The *RF* is computed using Eqn. 3.1

## 4. CASE STUDY

### 4.1. General Overview

A new steel frame building located in Lisbon, Portugal, is used in order to demonstrate the applicability of the proposed framework, considering the two sequences of events described above. Fig. 4.1 shows the steel moment frame used in this case study. The soil foundation type is assumed to be type A as per EC8 (IPQ, 2010b). Square hollow sections SHS300 are used in the columns and beams are executed with wide flange beams IPE360, both made of Steel S355. All floors have slabs with 0.20*m* thickness, which are unidirectional. In addition to the self-weight, the superimposed loads considered are as follows: on the 1st floor the load is 7.5$kN/m^2$ ($\psi_2$=0.8); on the 2nd and 3rd floors 3.0$kN/m^2$ ($\psi_2$=0.6) and 4.0$kN/m^2$ ($\psi_2$=0.3), respectively. The mass of the structure is assigned to the nodes, while the loads are uniformly distributed on the beams. A nonlinear finite element model of the structure which accounts for cyclic deterioration of components is developed in OpenSees (Mazzoni et al., 2009). A sequence of nonlinear dynamic time-history response analyses are performed using ten modified historical ground motions records obtained from the PEER NGA database (PEER, 2007). The analysis is performed considering $n_{sa_1^m}$ =18 mainshock spectral accelerations within cumulative probabilities between 0.18 and 0.9999.

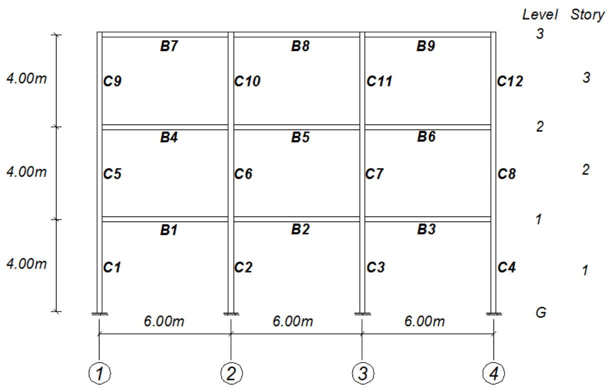


**Figure 4.1.** Steel Moment Resisting Frame

### 4.2. Structural Modelling

A nonlinear finite element model of the structure which accounts for cyclic deterioration of components behaviour is developed in this study. The force-based plastic hinge integration method proposed by Scott and Fenves (2006) is used through the application of the OpenSees *beamWithHinges* element. The model is intended to capture progressive collapse situations that result from propagation of localized damage on the structure. Model parameters of moment-rotation relationships of the plastic hinge regions, including the ones associated with the deterioration modes considered, are estimated through empirical relationships developed by Lignos (2008) and Lignos and Krawinkler (2011), which resulted from statistical treatment of hundreds of experimental tests performed over the last decades. The empirical information compiled by Lignos and Krawinkler (2011) can be assigned to any force-deformation relationship. The moment-rotation relationships that describe the rotation behavior of the plastic hinge section of both beams and columns are described following the models proposed by Lignos and Krawinkler (2007, 2011). The remaining parameters that characterize the deterioration model are defined according to the work of Ibarra and Krawinkler (2005). Furthermore, in order to simulate the real behaviour of the tri-dimensional structure after removing the base column, the stiffness and strength of beams perpendicular to the frame plan are also considered. To assess the contribution of the out-of-plane beams a pushdown analysis (Lu et al., 2012) of a 3-D subassembly was performed. The force-deformation that resulted from this pushdown analysis allow for the definition of a translational (vertical) spring that characterizes the behaviour of the out-of-plane beams.

P-Delta geometric transformation is used in the nonlinear analysis. Newton-Raphson method is used for numerical resolution of nonlinear equations and the Newmark constant acceleration method is used for time integration of the equations of motion. An eigenvalue analysis of the structure resulted in a fundamental period of $T_1$ = 0.91*s*. A Rayleigh damping with damping ratio of 2% assigned to the 1$^{st}$ and 6$^{th}$ modal frequencies (1.10*Hz* and 7.54*Hz*, respectively) is assumed.

## 4.3. Results

*4.3.1. Nonlinear dynamic time-history response analysis example including cascading events*

Results obtained from application of one of the nonlinear dynamic time-history response analyses of the structure subjected to a mainshock and cascading events are shown next. The results shown correspond to a case in which the mainshock is applied first, followed by removal of the column C1, and followed by the application of an aftershock. Fig. 4.2 shows the deformed shape of the structure at three instants during an analysis. Fig. 4.2(*a*) illustrates the deformed shape when the peak roof displacement is attained during the mainshock, Fig. 4.2(*b*) shows the deformed shape of the structure one second after the column C1 has been removed, and Fig. 4.2(*c*) illustrates the deformed shape at the instant when the peak roof displacement is achieved during the aftershock.

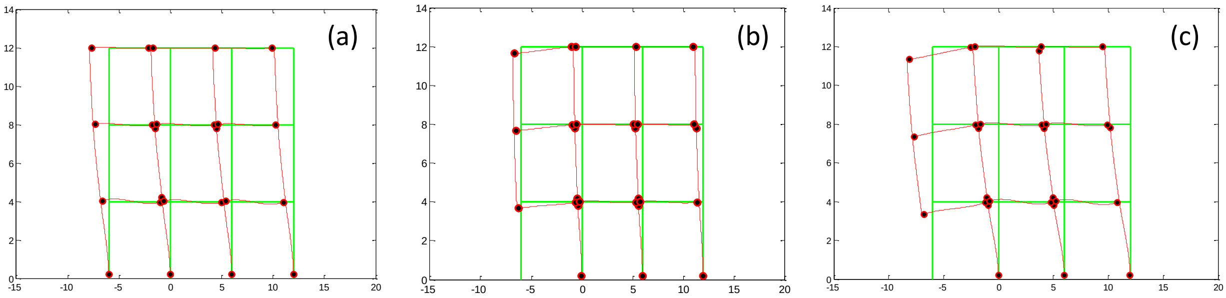


**Figure 4.2.** Deformed shape of the structure at instants when: (a) peak roof displacement during the mainshock is achieved; (b) 1s after the column C1 has been removed; and (c) maximum roof displacement during the aftershock

In addition, Fig. 4.3 shows the time-history of the horizontal displacement and also the vertical displacement of the top of column C1 (before and after the element removal). Fig. 4.3 shows the moments at the base of column C2 during the analysis.

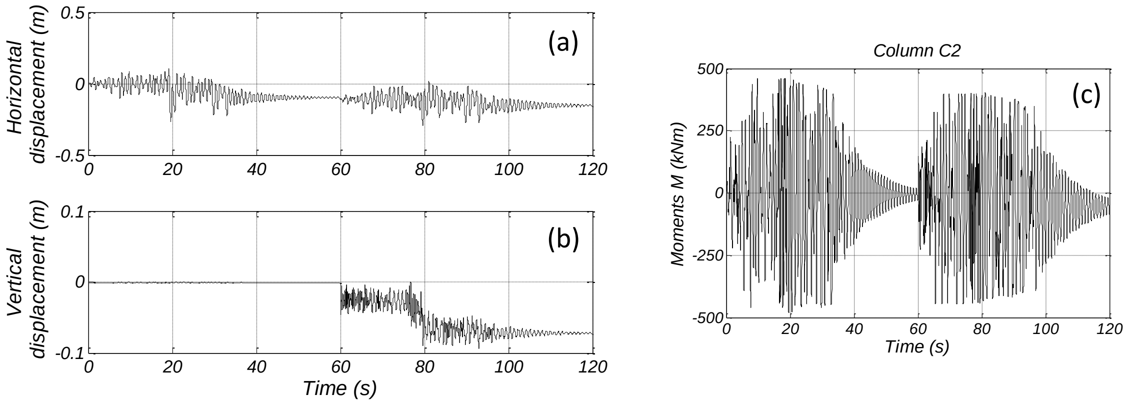


**Figure 4.3.** (a) Roof horizontal displacement above column C1; (b) Roof vertical displacement above column C1; and (c) Bending moments at base of column C2

*4.3.2. Final results*

Fig. 4.4 presents the mean results obtained after all mainshock $S_a^m(T_1)$ values and all real accelerograms considered had been analyzed. This figure shows the smallest aftershock spectral acceleration that reaches the collapse criteria, as a function of the mainshock spectral acceleration. For low mainshock intensities, there is no noticeable damage on the structure and, consequently, its spectral accelerations have little impact on risk. As the mainshock intensities increase the aftershock intensities that lead to structural collapse decrease. For larger intensities of the mainshock itself the structure would tend to collapse and the aftershock spectral accelerations would tend to zero. When columns are removed after the application of the mainshock, the spectral values of the aftershock that induce collapse also decrease.

If only one dynamic analysis was performed, i.e. the structure was subjected to the mainshock only, the mean spectral acceleration (out of the 10 earthquakes) leading to collapse is 2.23g for seismic action type 1 and 2.05g for type 2, and corresponds to a probability of collapse of $8.25 \times 10^{-5}$. Otherwise, the total collapse probabilities for all seismic triggered sequences of events considered are shown in Table 4.1.

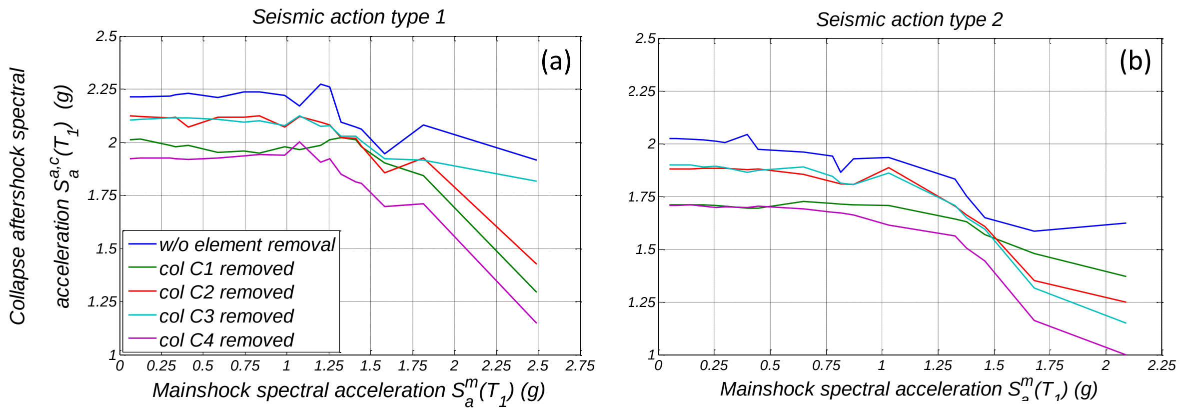


**Figure 4.4.** Mean aftershock spectral acceleration that leads the structure to collapse as a function of the mainshock spectral acceleration for: (a) seismic action type 1; and (b) seismic action type 2

**Table 4.1.** Collapse probabilities and robustness factors

| Events | Collapse probability ($P(C\|ds)$) | Robustness factor (*RF*) |
|---|---|---|
| Mainshock only | $8.25 \times 10^{-5}$ | 1.000 |
| Mainshock - aftershock | $2.26 \times 10^{-4}$ | 0.176 |
| Mainshock - column C1 removed due to fire/blast - aftershock | $2.97 \times 10^{-4}$ | 0.074 |
| Mainshock - column C2 removed due to fire/blast - aftershock | $2.75 \times 10^{-4}$ | 0.097 |
| Mainshock - column C3 removed due to fire/blast – aftershock | $2.80 \times 10^{-4}$ | 0.091 |
| Mainshock - column C4 removed due to fire/blast - aftershock | $3.29 \times 10^{-4}$ | 0.050 |

The second column in Table 4.1 lists the probability of collapse for the reference case (mainshock only) and for the post-mainshock scenarios considered. The results presented are obtained assuming a certain post-mainshock scenario, i.e. after the mainshock either an aftershock occurs or base column is removed and an aftershock occurs. If the probability of fire/blast post-mainshock is equal to 0.3 and assuming that all the four base column have equal probabilities of being damaged, the total probability of collapse, under these assumptions, computed through Eqn. 3.5, is $P(C) = 2.47 \times 10^{-4}$.

The third column in Table 4.1 presents the *RF* as computed using Eqn. 3.1. The *RF* is equal to one if the mainshock alone is applied to the structure, and the *RF* decreases in the probability of collapse associated with sequences of events.

## 5. CONCLUSIONS

In this study a new probabilistic framework methodology regarding post-mainshock risk scenarios is proposed. Special attention is given to sequences of events triggered by a mainshock. Due to the current state of knowledge a simplified probabilistic methodology for computation of the probabilities of collapse that accounts for the effects of fire/blasts and aftershocks was also presented. This methodology allows the study of the behavior of damaged structures in post-mainshock risk scenarios, which is not addressed in current codes.

The applicability of the proposed methodology was demonstrated through a case study of a steel frame building, which was designed according to EC3 (2010a) and EC8 (2010b). The structure was subjected to two specific sequences of events, namely mainshock followed by aftershock and mainshock followed by partial collapse of a structural element (simulating the occurrence of fire/blast) and aftershock. The nonlinear structural model implemented in OpenSees included a hysteretic model that accounts for cyclic deterioration of moment-rotation behavior in plastic hinge regions. Collapse probabilities were quantified for this case study. Results highlighted the importance of the consideration of these seismic triggered events in the robustness assessment. On the other hand, the different sequences of events considered showed that the inclusion of localized damage, such as the one induced by fire or blasts should be considered as it decreases the residual resistant capacity of the structure, when compared to the one associated with the occurrence of an aftershock that follows the mainshock.

Future developments of the present study should include correlation between the mainshock and aftershock as some studies have shown (e.g., Reasenberg and Jones (1989)). Furthermore, studies on fire or blasts effects and time-dependent capacity of structural components in OpenSees are also necessary.

## REFERENCES


Bartlett, J.E., Kotrlik, J.W., and Higgins, C. (2001). Organizational research: Determining appropriate sample size for survey research. *Information Technology, Learning, and Performance Journal*, **19(1):**43–50.

Bazzurro, P., Cornell, C., Menun, C., Motahari, M., and Luco, N. (2006). Advanced seismic assessment guidelines. Technical report, Pacific Earthquake Engineering Research Center - College of Engineering. PEER Report 2006/5.

Braxtan, N.L. and Pessiki, S.P. (2011). Postearthquake fire performance of sprayed fire-resistive material on steel moment frames. *Journal of Structural Engineering*, **137(9):**946–953.

Burden, R.L. and Faires, J.D. (1985). 2.1 The Bisection Algorithm. Numerical Analysis. PWS Publishers.

Campos-Costa, A., Sousa, M.L., and Oliveira, C.S. (1998). Seismic risk: Methods and application to portugal. In *11th European Conference on Earthquake Engineering*. Paris.

Faizian, M., Schalcher, H.R. and Faber, M.H. (2005). Consequence Assessment in Earthquake Risk Management using Damage Indicators. *Special issue of Int. Journal of Risk Assessment and Management*

Ibarra, L.F. and Krawinkler, H. (2005). Global collapse of frame structures under seismic excitations. Technical Report 152, The John A. Blume Earthquake Engineering Research Center, Department of Civil Engineering, Stanford University, Stanford, CA.

IPQ. NP EN 1993-1. (2010a). Eurocode 3 - Design of steel structures. Part 1-1: General rules and rules for buildings. Instituto Português da Qualidade.

IPQ. NP EN 1998-1:2010. (2010b). Eurocode 8 - Design of structures for earthquake resistance. Part 1: General rules, seismic actions and rules for buildings. Instituto Português da Qualidade.

Jayaram, N. and Baker, J. (2008). Statistical tests of the joint distribution of spectral acceleration values. *Bulletin of the Seismological Society of America 2008,* **98(5):**2231–2243.

JCSS (2001). Probabilistic model code. The Joint Committee on Structural Safety.

Lignos, D.G. (2008). Sidesway collapse of deteriorating structural systems under earthquake excitations. Ph.D. thesis, Department of Civil and Environmental Engineering, Stanford University, Stanford California.

Lignos, D.G. and Krawinkler, (2007). H. A database in support of modeling of component deterioration for collapse prediction of steel frame structures. *ASCE Structures Congress, Long Beach CA, SEI institute*.

Lignos, D.G. and Krawinkler, H. (2011). Deterioration Modeling of Steel Components in Support of Collapse Prediction of Steel Moment Frames under Earthquake Loading. *ASCE, Journal of Structural Engineering*, **137(11):**1291-1302

Lu, D., Cui, S., Song, P., and Chen, Z. (2012). Robustness assessment for progressive collapse of framed structures using pushdown analysis methods. *International Journal of Reliability and Safety*, **6(1):**15–37.

Luco, N., Bazzurro, P., and Cornell, C. (2004). Dynamic versus static computation of the residual capacity of a mainshock-damaged building to withstand an aftershock. In *13th World Conference on Earthquake Engineering*. Vancouver, Canada, 2004.

Luco, N., Gerstenberger, M.C., Uma, S., Ryu, H., Liel, A.B., and Raghunandan, M. (2011a). A methodology for post-mainshock probabilistic assessment of building collapse risk. In *Pacific Conference on Earthquake Engineering*. Auckland, New Zealand, April 2011.

Luco, N., Uma, S., Ryu, H., Liel, A.B., and Raghunandan, M. (2011b). Developing fragilities for mainshock-damaged structures through incremental dynamic analysis. In *Pacific Conference on Earthquake Engineering*. Auckland, New Zealand, April 2011.

Mardia, K. and Jupp, P. (2000). Directional Statistics (2nd edition). John Wiley and Sons Ltd.

Mazzoni, S., McKenna, F., Scott, M.H., and Fenves, G.L. (2009). The OpenSees command language manual, version 2.0. Pacific Earthquake Eng. Research Center, Univ. California at Berkeley.

McGuire, R.K. (2004). Seismic Hazard and Risk Analysis:Monograph MNO-10. EERI .

Moehle, J. and Deierlein, G. (2004). A framework methodology for performance-based earthquake engineering. In *13th World Conference on Earthquake Engineering*, Paper No. 679. Vancouver, BC, Canada.

Mukherjee, S. and Gupta, V. (2002). Wavelet-based generation of spectrum-compatible time-histories. *Soil Dynamics and Earthquake Engineering*, **22(9):**799–804.

Mukherjee, S. and Gupta, V. (*2007*). WAVGEN - Wavelet-Based Generation of Spectrum-Compatible Ground Motion. http://home.iitk.ac.in/ vinaykg/wavgen.htm.

Pacific Earthquake Engineering Research Center (2007). *NGA Database*,. www.peer.berkeley.edu/nga.

Scott, M.H. and Fenves, G.L. (2006). Plastic hinge integration methods for force-based beam-column elements. *Journal of Structural Engineering*, **132(2):**244–252.

Reasenberg, P. and Jones, L. (1989). Earthquake hazard after a mainshock in California. Science.

Ribeiro, F.L.A. (2011). Análise de Robustez de Estruturas Sujeitas a Eventos Sísmicos Consecutivos. Master Thesis. Faculdade de Ciências e Tecnologia – Universidade Nova de Lisboa. Lisboa, Portugal.

Talaat, M.M. and Mosalam, K.M. (2009). How to simulate column collapse and removal in as-built and retrofitted building structures? In Seismic Risk Assessment and Retrofitting, vol.10 of Geotechnical, Geological, and Earthquake Engineering, pages 427–452. Springer Netherlands. I. Alper, K. Faruk, P. Sumru, and Y. Ercan editors

Vamvatsikos, D. and Cornell, C. (2002). Incremental dynamic analysis. *Earthquake Engineering and Structural Dynamics*, **31(3):**491–514.

Yeo, G.L. and Cornell, C. (2005). Stochastic characterization and decision bases under time-dependent aftershock risk in performance-based earthquake engineering. Technical report, Pacific Earthquake Engineering Research Center - College of Engineering. PEER Report 2005/13.